
SUPPORTING INFORMATION

for

Interaction of amphiphilic polymer with medium-chain fatty alcohol to enhance rheological performance and mobility control ability

Yao Lu^{1,2}, Ziyu Meng¹, Kai Gao¹, Jirui Hou¹, Hairong Wu^{1,*}, Wanli Kang^{1,3,*}

¹ Research Institute of Enhanced Oil Recovery, China University of Petroleum (Beijing), Beijing, P.R. China 102249

² Department of Civil and Environmental Engineering, University of Alberta, Edmonton, Alberta, Canada T6G 2W2

³ School of Petroleum Engineering, China University of Petroleum (East China), Qingdao, Shandong, P.R. China 266580

* Corresponding authors: Wanli Kang, e-mail: kangwanli@upc.edu.cn, Tel.: +86-13589332193; Hairong Wu, e-mail: hrwu@cup.edu.cn, Tel.: +86-15010260120.

Basic parameters of polymer and crude oil

The basic parameters of HMPAM were determined according to the technical specifications of polymers for polymer flooding in China. The results are displayed in Table S1. The viscosity-average molecular weight of HMPAM was measured by Ubbelohde viscometer at 30°C as shown in Figure S1. Before measurement, excessive β -CD was added to the HMPAM solutions to shield the interference of the hydrophobic association by masking the hydrophobic groups. The following equations were employed.

$$\eta_r = t/t_0 \quad (1)$$

$$\eta_{sp} = \eta_r - 1 \quad (2)$$

Herein, t_0 is the flow time of the 1.0 M NaCl solution, s; t is the flow time of polymer solutions, s. The intrinsic viscosity ($[\eta]$) could be obtained by plotting η_{sp}/c and $\ln\eta_r/c$ as functions of concentration and taking the intercept. The obtained $[\eta]$ of HMPAM is 775.6 mL·g⁻¹,

corresponding to the viscosity-average molecular weight of $328 \times 10^4 \text{ g} \cdot \text{mol}^{-1}$ according to Mark-Houwink's experience formula. The CAC value was obtained from the viscosity-concentration curve of HMPAM. Moreover, the properties of the crude oil are also displayed in Table S2.

Table S1. Basic parameters of HMPAM.

Parameter	Value
Appearance	White powder
Degree of hydrolysis (%)	25
Hydrophobic monomer	N-hexadecylacrylamide
Hydrophobic monomer content (mol%)	1.0
CAC ($\text{mg} \cdot \text{L}^{-1}$)	930
Intrinsic viscosity ($\text{mL} \cdot \text{g}^{-1}$)	775.6
Molecular weight ($10^4 \text{ g} \cdot \text{mol}^{-1}$)	328
Solid content (%)	90.5
Dissolution time (h)	< 2

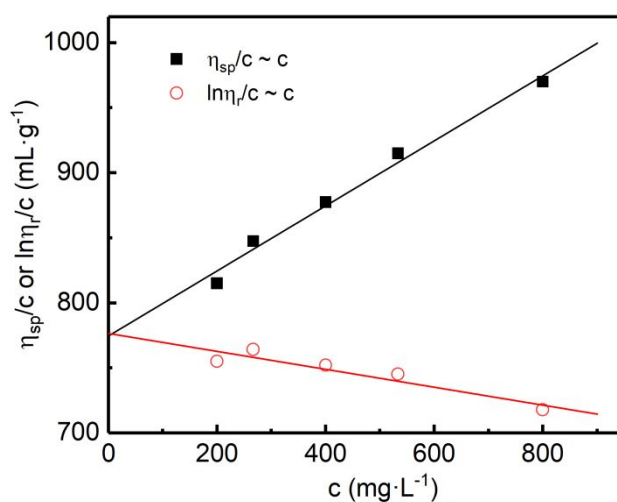


Figure S1. η_{sp}/c and $\ln \eta_r/c$ as functions of HMPAM concentration.

Table S2. Properties of the crude oil.

Properties	Values
Saturate (%)	80.31
Aromatics (%)	15.43
Resin (%)	4.25
Asphaltene (%)	0.01
Acid value (mg KOH/g)	0.07
Viscosity at 45°C (mPa·s)	5.3
Density at 30°C (g·cm ⁻³)	0.845

Shear recovery performance of HMPAM and HMPAM+C8OH

The viscosity as a function of shear rate and time for 1000 mg·L⁻¹ HMPAM+C8OH and 1000 mg·L⁻¹ HMPAM is shown in Figure S2. Both HMPAM and HMPAM+C8OH systems display the phenomenon of shear recovery due to the existence of hydrophobic association in both two systems.

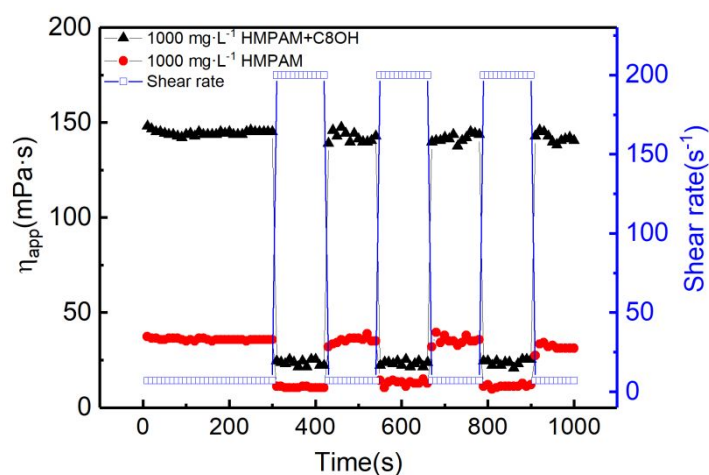


Figure S2. Viscosity as a function of shear rate and time for 1000 mg·L⁻¹ HMPAM+C8OH and 1000 mg·L⁻¹ HMPAM at 30 °C.

The hydrodynamic radius distribution and micromorphology

A Nano ZS90 laser particle analyzer (Malvern Instrument, UK) was employed to measure the hydrodynamic radius distribution at 30 °C. The machine was equipped with a He-Ne laser (633

nm) and based on the principle of dynamic light scattering. The scattering angle was fixed at 90°. The Hitachi S-4800 type cold field emission scanning electron microscopy (Hitachi Corp., Japan) was employed to observe the microstructures of HMPAM systems. The acceleration voltage is 5 kV.

One can see from Figure S3a that there are multi-peaks of hydrodynamic radius for both HMPAM and HMPAM+C8OH systems. For the 1000 mg·L⁻¹ HMPAM without C8OH, the first peak at $R_h=25.8$ nm is indicative of the intramolecular hydrophobic association while the second peak at $R_h=126.8$ nm is indicative of the intermolecular hydrophobic association. In contrast, for the combined system of HMPAM+C8OH, the initial peak at $R_h=25.8$ nm almost diminishes and the other two peaks appear at $R_h=107.6$ nm and $R_h=598.4$ nm. Furthermore, as shown in Figure S3b and Figure S3c, the denser reticular structure could be observed in HMPAM+C8OH compared to HMPAM with the same polymer concentration of 1000 mg·L⁻¹.

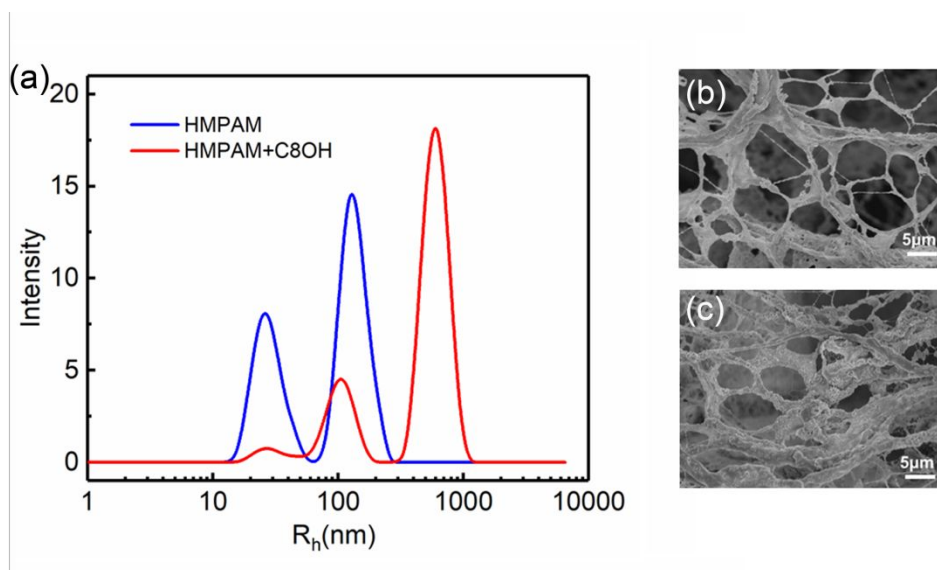


Figure S3. (a) The hydrodynamic radius distribution of HMPAM and HMPAM + C8OH; (b) SEM image of HMPAM; (c) SEM image of HMPAM + C8OH. HMPAM concentration = 1000 mg·L⁻¹; C8OH concentration = 750 mg·L⁻¹.

Effect of octane concentration on HMPAM viscosity

Figure S4 shows the effect of octane concentration on HMPAM viscosity. One can see that the significant increase of viscosity does not occur when we interchange the C8OH with octane. It indicates that the hydroxyl of C8OH is indispensable for facilitating the re-aggregation of

association structure. The hydrogen bond could be formed between the hydroxyl of C8OH and the carboxylate of HMPAM backbone.

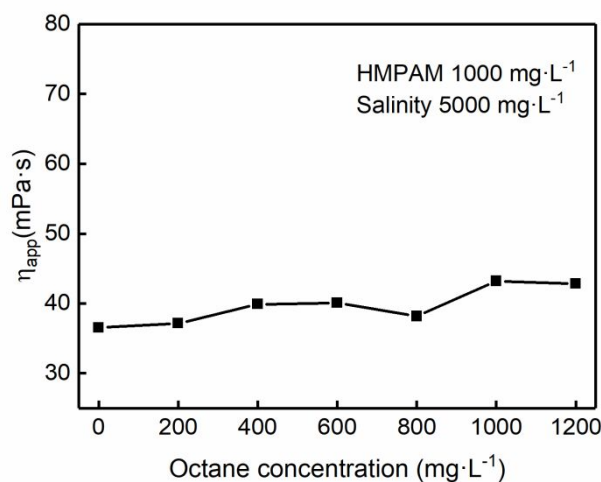


Figure S4. Effect of octane concentration on HMPAM viscosity at 30 °C.

Aging stability of HMPAM and HMPAM+C8OH

One can see from Figure S5 that the viscosity of both 2000 mg·L⁻¹ individual HMPAM and 1000 mg·L⁻¹ HMPAM + 750 mg·L⁻¹ C8OH decreases in 15 days at 45 °C because of the degradation of a small amount of HMPAM. However, there is no sudden viscosity drop in HMPAM+C8OH, indicating that the system could keep long-term stability in reservoir conditions.

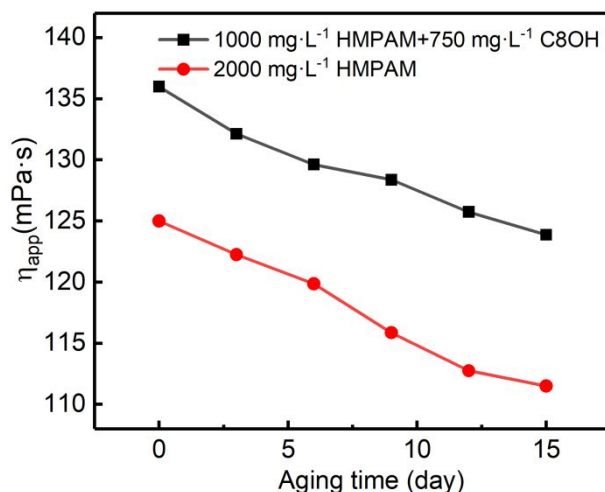


Figure S5. Apparent viscosity of HMPAM and HMPAM+C8OH systems as a function of aging time at 45 °C. Salinity = 5000 mg·L⁻¹; shear rate=7 s⁻¹.

Emulsification performance of HMPAM and HMPAM+C8OH

The crude oil from Changqing oilfield was employed in the emulsification tests. The prepared polymer aqueous solution and crude oil (7:3, v/v) were first added in a vial. The vial was then quickly shaken up and down for 20 times, and the phase separation was recorded. Figure S6 shows the emulsification results of three different systems. It can be seen that the crude oil emulsion could not be well stabilized by $1000 \text{ mg}\cdot\text{L}^{-1}$ HMPAM and a clear oil-water interface is observed after 2 hours (see Figure S6b). In contrast, the emulsion stabilized by $1000 \text{ mg}\cdot\text{L}^{-1}$ HMPAM+ $750 \text{ mg}\cdot\text{L}^{-1}$ C8OH or $2000 \text{ mg}\cdot\text{L}^{-1}$ HMPAM separates with a much slower rate (see Figure S6a and c, respectively). The better emulsifying ability of HMPAM+C8OH could be due to the enhancement of interfacial adsorption and bulk viscoelasticity in presence of C8OH.

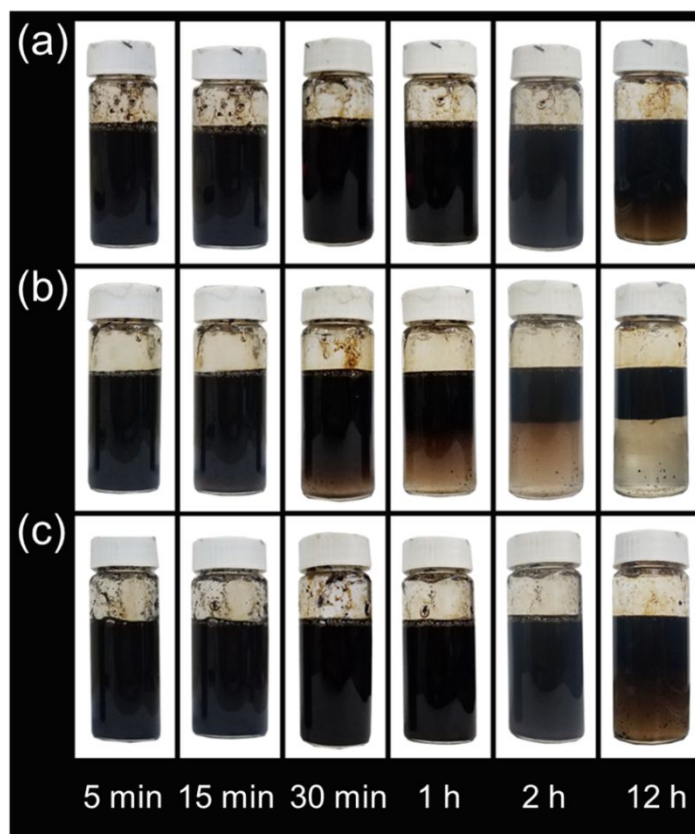


Figure S6. Crude oil emulsions stabilized by (a) $1000 \text{ mg}\cdot\text{L}^{-1}$ HMPAM+ $750 \text{ mg}\cdot\text{L}^{-1}$ C8OH, (b) $1000 \text{ mg}\cdot\text{L}^{-1}$ HMPAM and (c) $2000 \text{ mg}\cdot\text{L}^{-1}$ HMPAM.